Available online at www.sciencedirect.com
SCIENCE DIRECT®
Thermochimica Acta 431 (2005) 182–187
thermochimica acta
www.elsevier.com/locate/tca

Water behavior in the conversion process of gel-to-subgel phase in dimyristoylphosphatidylethanolamine–water system as studied by DSC

H. Aoki, M. Kodama *

Department of Biochemistry, Faculty of Science, Okayama University of Science, 1-1 Ridai-cho, Okayama 700-0005, Japan

Received 9 November 2004; received in revised form 16 February 2005; accepted 19 February 2005
Available online 23 May 2005

Abstract

The gel phase of dimyristoylethanolamine (DMPE)–water system was annealed at temperatures of −5 to +5 °C for periods of 2 weeks and was converted into a more stable state of the so-called *L*-subgel phase. To elucidate the role of water molecules in the conversion of the gel to the subgel phase, the ice-melting behavior for the DMPE–water samples of varying periods of the annealing was investigated by a differential scanning calorimetry (DSC). The ice-melting DSC curves were deconvoluted according to a computer program for multiple Gaussian curve analysis, and the numbers of freezable interlamellar and bulk water molecules were estimated from respective ice-melting enthalpies of the deconvoluted curves. At the annealing periods of 4 days, water molecules amounting to 3.5 H_2O/lipid were observed to be further incorporated into regions between the bilayers, giving rise to the total number of freezable interlamellar water molecules 7 H_2O/lipid which is fairly larger than that (4 H_2O/lipid) estimated for the gel phase. Finally, the conversion of the gel-to-subgel phases completed at the annealing periods of 10 days. The resultant subgel phase showed the amount of nonfreezable interlamellar water larger by 1 H_2O/lipid than that of the nonannealed gel phase. Furthermore, the present study indicated an essential role of the bulk water molecules, which fill an empty space produced at the lipid bilayer surface in the conversion process of the gel-to-subgel phases.
© 2005 Elsevier B.V. All rights reserved.

Keywords: DSC; DMPE–water system; Subgel phase; Interlamellar water molecule; Deconvolution analysis

1. Introduction

Phospholipids are major components of biomembranes and constitute a fundamental part of their bilayer structure. To date, many studies on the stability for the gel phase of lipid–water systems have been performed for various phospholipids [1–16], and it has become apparent that the gel phase is metastable and converts to a more stable phase, generally called a subgel phase when the thermal annealing adopted for the gel phase is adequate. In this respect, it has been reported that the subgel phase of dimyristoylphosphatidylethanolamine (DMPE)–water system is present in two types designated as the *L*- and *H*-subgel phases which appear, respectively, at temperatures lower and higher than the gel-to-liquid crystal transition [17–21]. In previous studies on the subgel phase, much attention of investigations has been paid to a lateral packing of the lipid molecules in an intrabilayer. However, in our previous paper [16,19,21,22], we have pointed out an important role of water molecules in the conversion of the gel-to-subgel phases.

From this viewpoint, focusing on the *L*-subgel phase, the present study investigated the role of water molecules in the conversion of the gel to the subgel phase in the DMPE–water system. In this study, the ice-melting DSC curves were measured for the samples of varying periods of annealing. To estimate the numbers of freezable interlamellar and bulk water molecules, a deconvolution analysis of the ice-melting DSC curves was performed according to a computer program of Gaussian curve analysis.

2. Experimental techniques

2.1. Materials and preparation of samples

1,2-Dimyristoyl-3-*sn*-phosphatidylethanolamine was purchased from Sigma and used without further purification.

* Corresponding author. Fax: +81 86 255 7700.
E-mail address: kodama@dbc.ous.ac.jp (M. Kodama).

0040-6031/$ – see front matter © 2005 Elsevier B.V. All rights reserved.
doi:10.1016/j.tca.2005.02.037

The DMPE in a high-pressure crucible cell (Mettler differential scanning calorimeter) was dehydrated under high vacuum (10^{-4} Pa) at room temperature. The crucible cell containing the dehydrated DMPE was sealed off in a dry box filled with dry N_2 gas and was then weighted by a microbalance. A series of samples of varying water contents ranging in water/lipid molar ratio (N_w) from 10.0 to 15.8 was prepared by adding the desired amounts of water to the dehydrated DMPE (∼30 mg) with a microsyringe. The gel phase samples were prepared as follows: the mixtures of DMPE and water at varying water contents were maintained at temperatures above the gel-to-liquid crystal phase transition until the same transition behavior was attained. The gel phase samples thus obtained were converted to the *L*-subgel phase by an annealing of repeating thermal cycling at temperatures of −5 to 5 °C at a rate as slow as 0.2 °C min^{-1} over period of 2 weeks (this annealing condition was confirmed by us to complete the conversion of the gel to the *L*-subgel phase [19]).

2.2. Differential scanning calorimetry

A DSC was performed with a Mettler TA-4000 apparatus for a sample in the high-pressure crucible cell and on heating from −60 °C to temperatures of the liquid crystal phase at a rate of 0.5 °C min^{-1}. The DSC for the gel samples was performed by cooling the liquid crystal samples directly from 70 to −60 °C, and for the subgel samples obtained by the annealing the DSC was initiated by cooling them directly from 70 to −60 °C. Furthermore, to make clear the process of conversion of the gel to the *L*-subgel phase, the DSC was performed for a fully hydrated sample at N_w 13.9 for each 1.5 days during the annealing period of 2 weeks.

2.3. Deconvolution analysis of ice-melting DSC curves

The ice-melting DSC curves of varying water contents were separated into two components for freezable interlamellar and bulk water by a deconvolution analysis because the two components overlap at their basis. The present deconvolution was performed according to a computer program for multiple Gaussian curve analysis under the following conditions: (1) the number of deconvoluted curves is minimal; (2) the theoretical curve given by the sum of individual deconvoluted curves is best fitted to the experimental DSC curve; (3) both the midpoint temperature and the half height–width (i.e., characterizing the van't Hoff enthalpy) for each of the deconvoluted curves are maintained almost constant throughout all the deconvolutions for varying water contents [11,16].

3. Results and discussions

Fig. 1 shows a series of DSC curves for the annealed samples of the DMPE–water system at varying water contents of $10.0 < N_w < 15.6$. In this figure, DSC curves of the annealed and nonannealed samples are compared at N_w 10.0 and are shown in (a) and (b), respectively. When these DSC curves are compared, a distinct difference is observed not only in the lipid phase transition behavior but also in the ice-melting behavior. As shown in Fig. 1a, the annealed sample shows multiple peaks at around 43 °C due to the phase transition of the *L*-subgel-to-gel phases, which is successively followed by the gel-to-liquid crystal phase transition at 50 °C. However, when a rescan is performed, no peak of the *L*-subgel-to-gel phase transition is observed, thus, the thermal behavior is the same as that for the nonannealed sample shown in Fig. 1b. The same result was obtained for other samples at different water contents of N_w 12.1, 13.9, and 15.6.

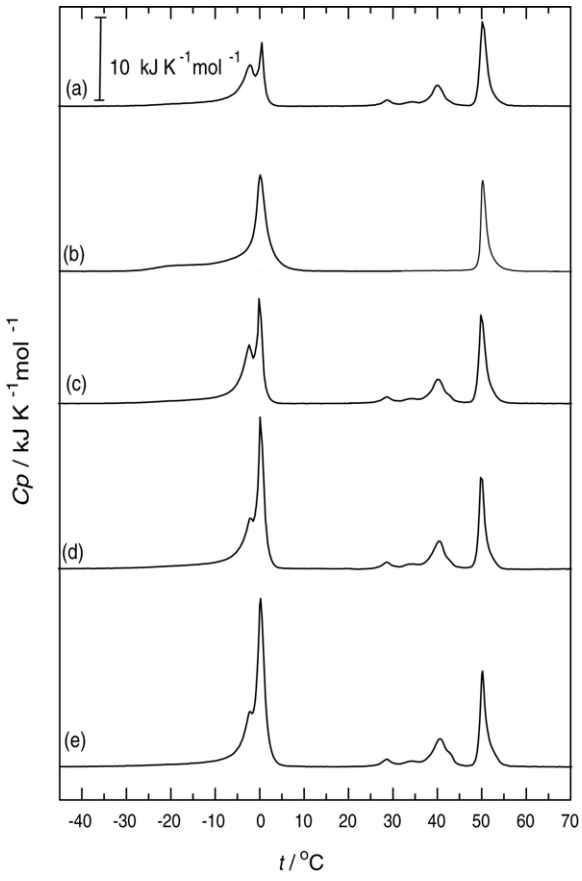

Fig. 1. A series of DSC curves of the DMPE–water system for annealed samples at N_w values of (a) 10.0, (c) 12.1, (d) 13.9, and (e) 15.6. Nonannealed sample at N_w 10.0 is shown in (b).

In order to make clear the difference between the ice-melting DSC curves (a) and (b) of Fig. 1, these curves are compared in an enlarged scale shown in Fig. 2a and b. In this regard, our previous studies have revealed that freezable water of the lipid–water system is present in two types, freezable interlamellar and bulk water. The freezable interlamellar water exists in regions between the lipid bilayers but keeps the degree of freedom necessary to form icelike hydrogen bonds with neighboring water molecules. The bulk water exists outside the bilayers and forms hexagonal-like ice on cooling. As shown in Fig. 2b, the nonannealed gel sample shows

the ice-melting DSC curve characteristic of the lipid–water system. Thus, the melting behavior of ice derived from the freezable interlamellar water is observed over a wide temperature range of −35 to about 0 °C, after which a sharp peak due to the melting of ice obtained from the bulk water appears at around 0 °C. In this contrast, for the annealed *L*-subgel sample, the melting of ice for the freezable interlamellar water occurs in a narrow temperature range of −20 to about 0 °C and is characterized by a shoulder peak, which is located at a foot of the sharp peak for the bulk water, as shown in Fig. 2a. Similarly, the ice-melting behavior of the annealed samples at varying water contents was characterized by the shoulder peak and the following sharp peak, as shown in Fig. 1c–e.

In the present study, we used the samples at water contents above N_w 10.0, at which a full hydration is reached. This is because all of the gel phase is not converted into the *L*-subgel phase by the annealing unless the sample is fully hydrated. Thus, some of the gel phase converts into the most stable *H*-subgel phase, which is transformed directly to the liquid crystal phase on heating.

As is shown in Fig. 1, the shoulder peak and the sharp peak composed of the ice-melting DSC curve for the annealed sample overlap at their basis, and so the two peaks were separated by a deconvolution analysis, in order to estimate the number of nonfreezable interlamellar, freezable interlamellar, and bulk water molecules for the *L*-subgel phase. The nonfreezable interlamellar water is defined as water, which cannot form ice-like hydrogen bonds even when cooled to extremely low temperatures. Fig. 2a shows a result of the deconvolution for the sample at N_w 10.0. For comparison, Fig. 2b exhibits a result for the nonannealed gel sample at the same water content. In this figure, deconvoluted ice-melting curves are shown by dotted lines. The shoulder peak for the freezable interlamellar water was further deconvoluted into three components with a view to performing the deconvolution as accurately as possible. Accordingly, deconvoluted curves I–III shown in Fig. 2a for the *L*-subgel phase are derived from the freezable interlamellar water and a deconvoluted curve IV derived from the bulk water. The ice-melting enthalpy ΔH_I for the freezable interlamellar was estimated from the deconvoluted curves I–III, and the ice-melting enthalpy ΔH_B for the bulk water estimated from the deconvoluted curve IV. In Fig. 3, the resultant ΔH_I and ΔH_B values for the *L*-subgel phase of varying water contents are plotted against N_w. For comparison, the ΔH_I and ΔH_B curves (dotted lines) for the gel phase previously reported by us [11,16] are added in Fig. 3. When the ΔH_I curve in Fig. 3 is compared between the *L*-subgel and gel phases although the compari-

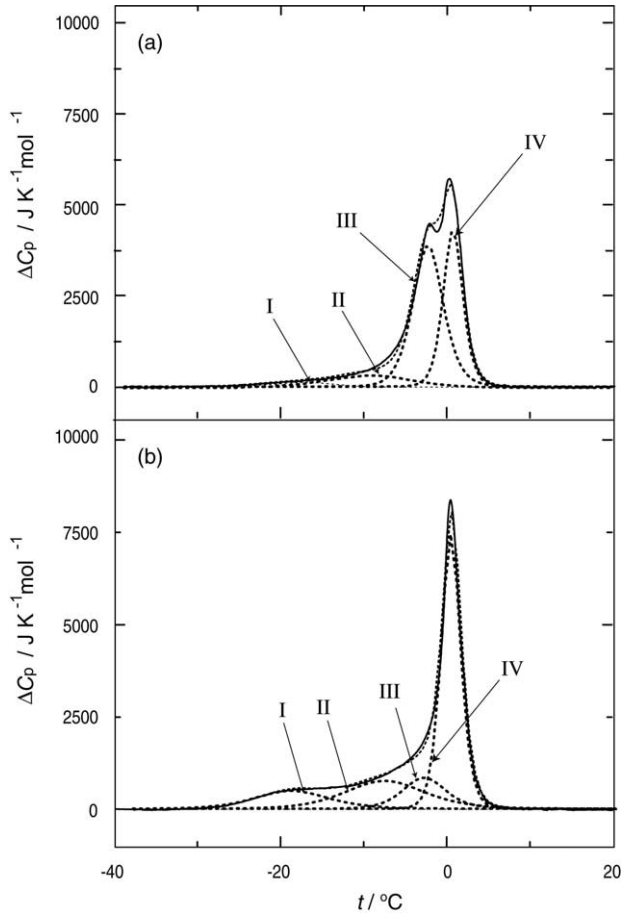

Fig. 2. Comparison of ice-melting DSC curves (solid lines) between (a) annealed sample (*L*-subgel) and (b) nonannealed sample (gel phase) of the DMPE–water system at the same water content of N_w 10.0. The deconvoluted curves I–IV and their sum (theoretical curve) are shown by dotted lines.

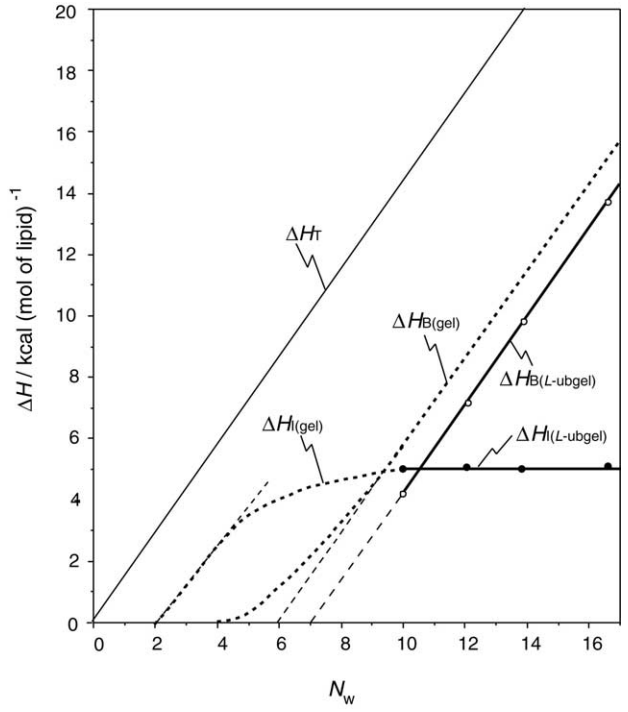

Fig. 3. The ice-melting enthalpies (solid lines), ΔH_B, ΔH_I, and ΔH_T, for the *L*-subgel phase of the DMPE–water system are plotted against N_w and are compared with those (dashed lines) for the gel phase previously reported by us [11]. ΔH_B: the ice-melting enthalpy for the bulk water per mole of lipid; ΔH_I: the ice-melting enthalpy for the freezable interlamellar water per mole of lipid; ΔH_T: the ice-melting enthalpy per mole of lipid obtained by assuming that all the water added to a sample is present as free water.

son is limited to water content above N_w 10, the curve of the *L*-subgel phase shows a good accordance with that of the gel phase. However, the ΔH_B curve of the *L*-subgel phase is parallel to that of the gel phase but the former is lowered by about 5.9 kJ/mol lipid compared with the later. These facts indicate that for a full hydration (i) the amount of the freezable interlamellar water is the same for the *L*-subgel and gel phases, but (ii) the amount of the bulk water for the *L*-subgel phase is smaller by approximately 1 H_2O/lipid than that for the gel phase, and (iii) consequently, the amount of nonfreezable water is larger by 1 H_2O/lipid for the *L*-subgel phase than for the gel phase. 1 H_2O/lipid for the nonfreezable water is assumed to exist in regions between adjacent lipid headgroups as the nonfreezable interlamellar water of the *L*-subgel phase. In this connection, our previous paper has revealed that for the fully hydrated gel phase the maximum number of nonfreezable interlamellar and freezable interlamellar water molecules is 2 H_2O and 4 H_2O per molecule of lipid, respectively [11,16]. Accordingly, the maximum number of nonfreezable interlamellar and freezable interlamellar water molecules of the L-subgel phase is calculated to be 3 H_2O and 4 H_2O per molecule of lipid, respectively.

Focusing on the above-discussed result, thus, the conversion of the gel-to-*L*-subgel phases by the annealing accompanies the structural change of water molecule from the freezable to nonfreezable water, the DSC was performed for the samples (N_w 13.9) annealed for varying period up to 2 weeks. In Fig. 4, typical DSC curves of varying periods of the annealing are compared. As shown in Fig. 4, the *L*-subgel-to-gel transition peak grows with increasing the annealing period up to 10 days, after which the limiting, saturated transition peak is observed. On the other hand, the shoulder peak (for the freezable interlamellar water), which is located at a foot of the sharp ice-melting peak (for the bulk water) at around 0 °C, becomes larger up to 3.5 days and then becomes smaller up to 10 days. This phenomenon is more clearly recognized by enlarged scale ice-melting peaks shown in Fig. 5. In this figure, results of the deonvolution analysis are also added. The number of freezable interlamellar water molecules, N_I, per molecule of lipid was estimated from ΔH_I (kJ/mol lipid)/5.35 (kJ/mol H_2O), where ΔH_I is given by the sum of individual enthalpy changes of the deconvoluted curves I–III, and 5.35 is the average ice-melting enthalpy per mole of H_2O present as the freezable interlamellar water. The average molar ice-melting enthalpy was obtained by a slope of linear portion ($2 < N_w < 4$) of the ΔH_I (gel) curve shown in Fig. 3. On the other hand, the number of the bulk water molecules, N_B, per molecule of lipid was estimated from ΔH_B (kJ/mol lipid)/5.94 (kJ/mol H_2O), where ΔH_B is given by the enthalpy change of deconvoluted curve IV, and 5.94 is an average molar ice-melting enthalpy of the bulk water obtained from a slope of the linear ΔH_B (gel) curve (and/or ΔH_B (*L*-subgel) curve) shown in Fig. 3.

Fig. 6 shows variations of N_B and N_I with increasing the period of annealing, together with the total number of freezable water molecules, denoted as N_{IB}, given by $N_I + N_B$. In this figure, the N_I curve shows a maximum at the annealing period of 4 days, in contrast to a minimum observed for the N_B curve. At this stage, the number of the freezable interlamellar water molecules reaches 7.5 H_2O/lipid, indicating that water molecules amounting to 3.5 H_2O/lipid are further incorporated into regions between the bilayers. In this contrast, the number of bulk water molecules is decreased by about 3.5 H_2O/lipid. After that, a decrease of the N_I curve with the annealing period is observed up to 10 days, in contrast to an increase observed for the N_B curve. Finally, for the resultant *L*-subgel phase, the N_I value becomes the same as that (4.0 H_2O/lipid) of the nonannealed gel sample (the annealing period of 0 days) and the N_B value reaches approximately 4.2 H_2O/lipid, which is less by 1 H_2O/lipid than that of the nonannealed gel sample. In this accord, the N_{IB} value of *L*-subgel phase is less by about 1 H_2O/lipid compared with that of the gel phase, as shown in Fig. 6. Accordingly, the number of nonfreezable interlamellar water molecules for the *L*-subgel phase increases by about 1 H_2O per molecule of lipid, compared with that for the gel phase.

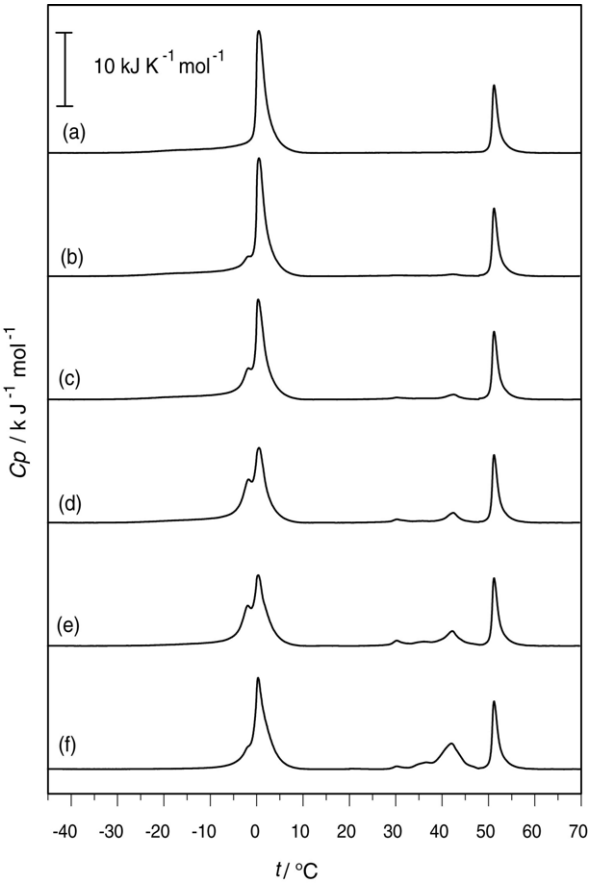

Fig. 4. Variation of DSC curves of the DMPE–water system with increasing a period of annealing up to 10 days. Annealing periods (day): (a) 0, (b) 1.5, (c) 2.5, (d) 3.4, (e) 6.0, and (f) 10.

A point to note in Fig. 6 is that additional uptake of freezable interlamellar water occurs in the conversion process of the gel-to-*L*-subgel phases and so at this stage the amount of this water is about two times larger than that of the gel phase.

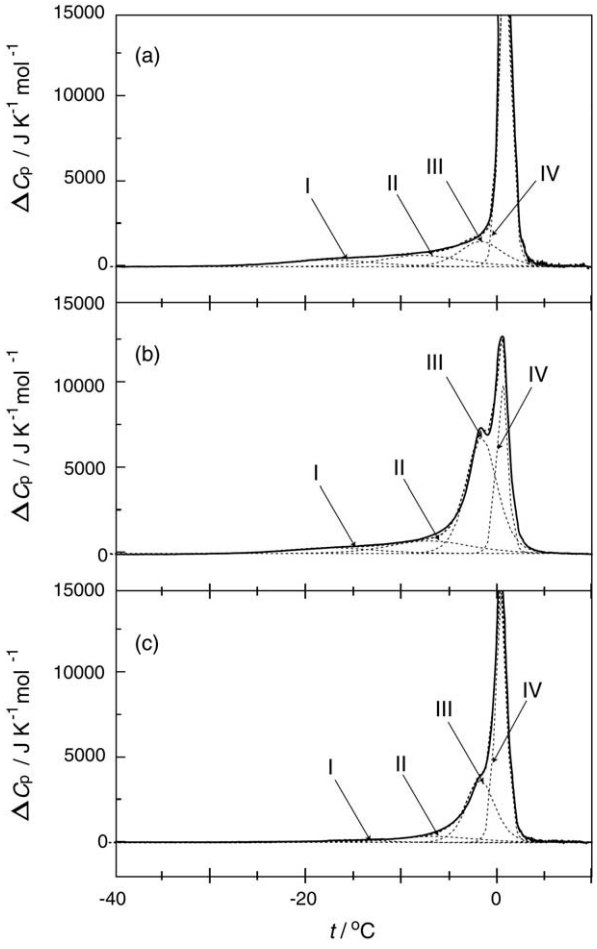

Fig. 5. Comparison of typical ice-melting DSC curves (solid lines) observed in the conversion process of the gel-to-*L*-subgel phases of the DMPE–water sample at N_w 13.9. The deconvoluted curves I–IV and their sum (the theoretical curve) are shown by dotted lines. Annealing periods (day): (a) 0, (b) 3.4, and (c) 10.

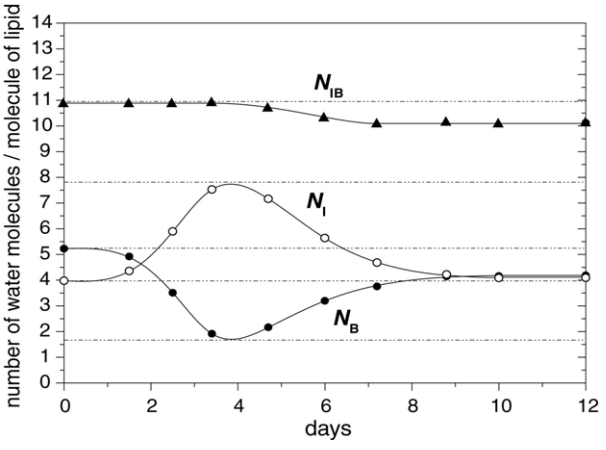

Fig. 6. Variations of N_B, N_I, and N_{IB} with increasing a period of annealing up to 10 days. N_B: the number of bulk water molecules per molecule of lipid; N_I: the number of freezable interlamellar water molecules per molecule of lipid; N_{IB}: the total number of freezable water molecules per molecule of lipid, given by $N_B + N_I$.

As is well known, the lipid molecules of the so-called subgel phase are more closely together packed than those of the gel phase, indicating that the van der Waals interaction operating between their hydrocarbon chains is stronger for the former than for the later. Accordingly, at a first stage of the conversion process, rearrangements of the lipid molecules to more closely packed states would take place in an intrabilayer. Such a rearrangement of the lipid molecules would induce an empty space at the bilayer surface of lipid molecules, so that this space would be filled by an infusion of bulk water existing outside the bilayer. So, both the maximum of the N_I curve and the minimum of the N_B curve are observed simultaneously at the annealing period of 4 days (Fig. 6). This result indicates an essential role of the bulk water molecules, which fill the empty space of the lipid bilayer surface in the conversion process of the gel-to-*L*-subgel phases. At a final stage of the conversion, the rearrangement of lipid molecules to a closer packing would be accomplished. This would accompany a release of freezable interlamellar water, resulting in a decrease in N_I, simultaneously with an increase in N_B, which is observed over the annealing period of 5–10 days.

Acknowledgements

This work is supported in part by Grants-in-Aid for General Scientific Research (12640568) from Ministry of Education, Science and Culture, Japan (2001), and by “High-Tech Research Center” Project for Private Universities: matching fund subsidy from MEXT (Ministry of Education, Culture, Sports, Science and Technology), 2004.

References

[1] M.J. Ruocco, G. Shipley, Biochim. Biophys. Acta 691 (1982) 309–312.
[2] M. Kodama, Thermochim. Acta 109 (1986) 81–93.
[3] M. Kodama, H. Hashigami, S. Seki, J. Colloid Interface Sci. 117 (1987) 497–509.
[4] M. Kodama, H. Inoue, Y. Tsuchida, Thermochim. Acta 266 (1995) 373–385.
[5] M. Kodama, H. Kato, H. Aoki, Thermochim. Acta 352 (2000) 213–227.
[6] M. Kodama, H. Aoki, T. Miyata, Biophys. Chem. 79 (1999) 205–219.
[7] S.C. Chen, J.M. Sturtevent, B.J. Gaffeny, Proc. Natl. Acad. Sci. U.S.A. 77 (1980) 5060–5063.
[8] H.H. Mantsch, S.C. Hsi, K.W. Butler, D.G. Cameron, Biochim. Biophys. Acta 728 (1983) 325–330.
[9] D.A. Wilkinson, T.J. McIntosh, Biochemistry 25 (1986) 295–298.
[10] R.M. Epand, B. Gabel, R.F. Epand, A. Sen, S.W. Hui, A. Muga, W.K. Surewicz, Biophys. J. 63 (1992) 327–332.
[11] M. Kodama, H. Aoki, H. Takahashi, I. Hatta, Biochim. Biophys. Acta 1329 (1997) 61–72.
[12] G. Klose, B. Konig, H.W. Meyer, G. Schulze, G. Degovics, Chem. Phys. Lipids 47 (1988) 225–234.
[13] K. Gawrisch, W. Richter, W.A. Mops, P. Balgavy, K. Arnold, G. Klose, Studia Biophys. 108 (1985) 5–16.

[14] R.N. Lewis, R.N. McElhaney, Biophys. J. 64 (1993) 1081–1096.
[15] J.F. Nagle, R. Zhang, T. Stephanie-Nagle, W. Sun, H.I. Petrache, R.M. Suter, Biophys. J. 70 (1996) 1419–1431.
[16] M. Kodama, H. Aoki, in: N. Garti (Ed.), Thermal Behavior of Dispersed Systems, Marcel Dekker Inc., New York, 2000, p. 247.
[17] S. Mulukutla, G.G. Shipley, Biochemistry 23 (1984) 2514–2519.
[18] D.A. Wilkinson, J.F. Nagle, Biochemistry 23 (1984) 1538–1541.
[19] H. Aoki, M. Kodama, J. Therm. Anal. 49 (1997) 839–858.
[20] H. Aoki, T. Koto, M. Kodama, J. Therm. Anal. Calorim. 64 (2001) 299–306.
[21] H. Aoki, M. Kodama, Thermochim. Acta 308 (1998) 77–83.
[22] M. Kodama, H. Kato, H. Aoki, J. Therm. Anal. Calorim. 64 (2001) 219–230.